

Photoemission properties of GaAs (100) $\beta_2(2\times 4)$ and GaAs (100) (4×2) reconstruction phases

Xiaohua Yu (鱼晓华), Zhonghao Ge (葛仲浩), and Benkang Chang (常本康)*

*Institute of Electronic Engineering and Opto-Electric Technology,
Nanjing University of Science and Technology, Nanjing 210094, China*

*Corresponding author: bkchang@mail.njust.edu.cn

Received January 29, 2013; accepted March 2, 2013; posted online July 17, 2013

Using the first-principles plane-wave pseudopotential method, based on the density function theory, the electron structure and optical properties of GaAs (100) $\beta_2(2\times 4)$ and GaAs (100) (4×2) reconstructions are calculated. The formation energy of As-rich $\beta_2(2\times 4)$ reconstruction is minus and the formation energy of Ga-rich (4×2) reconstruction is positive; As-rich $\beta_2(2\times 4)$ reconstruction is stable and Ga-rich (4×2) reconstruction is unstable. Ga-rich (4×2) reconstruction owns lower work function. The electrons at two reconstructions both move into the bulk and form a band-binding region. Both the absorption and the reflectivity of As-rich $\beta_2(2\times 4)$ reconstruction are smaller than the Ga-rich (4×2) reconstruction. As-rich $\beta_2(2\times 4)$ reconstruction is more benefit for the movement of photos through the surface to emit photoelectrons.

OCIS codes: 160.4760, 250.1500, 300.6170.

doi: 10.3788/COL201311.S21602.

GaAs is a new semiconductor material in the manufacture of microelectronics appliance and photoelectron appliance. With direct energy, band gap, GaAs owns many excellent performances that Si-based semiconductor material dose not have. With excellent performance, such as high sensitivity, low dark current, concentrated electron emission energy, and high quantum efficiency, negative electron affinity (NEA) GaAs photocathode activated by the adsorption of cesium and oxygen is widely applied in the weak light detection field^[1-4]. During the Cs/O activation, the surface of GaAs substrate is atomically clean. Relaxation and reconstructed would happen at the atomically clean GaAs surface because atoms at one side of the surface are disappeared.

For different reconstructions, different surface morphology and properties would lead to different photoelectric emission performance, GaAs (100) surface owns excellent photoelectric emission performance^[5]. The reconstruction phases can be divided into As-rich reconstruction phases and Ga-rich reconstruction phases. The As-rich reconstruction phases contain $c(4\times 4)$, $\gamma(2\times 4)$, $\beta_1(2\times 4)$, $\beta_2(2\times 4)$, $\alpha_1(2\times 4)$, and $\alpha_2(2\times 4)$ ^[6], and the Ga-rich reconstruction phases contain (4×2) , (4×6) ^[7], and so on. As-rich (2×4) phase grown by molecular beam epitaxy (MBE) is widely used in the Cs/O activation. Before the activation, high temperature clean process is used to get atomically clean surface. During this process relatively high temperature (650 °C) is taken to wipe off the gallium oxide and arsenious oxide. In this case, the As-rich (2×4) phase will turn to Ga-rich (4×2) phase. In this letter, the formation energy, work function, density of state, and optical properties of As-rich $\beta_2(2\times 4)$ phase and Ga-rich (4×2) phase are calculated, and the stability and photoelectric emission properties of these two reconstructions are compared. It has directing significance for GaAs photoelectric cathode.

The calculations in this letter are performed by the first-principles plane-wave pseudopotential method,

which is based on the first principle density functional theory (DFT)^[8,9]. The Broyden-Fletcher-Goldfarb-Shanno (BFGS) algorithm is used to optimize the reconstruction surface models. Slab model^[10] is taken in the calculation of As-rich $\beta_2(2\times 4)$ reconstruction phase and Ga-rich (4×2) reconstruction phase. GaAs (100) surface is got by cleaving (100) surface on the optimized GaAs conventional cell. After modifying atoms, As-rich $\beta_2(2\times 4)$ model and Ga-rich (4×2) model are built respectively. The reconstruction surface slabs are modeled with 7 layers of atoms (three Ga layers and four As layers). The top four layers are relaxed freely and the bottom three layers are fixed at the ideal positions to simulate a bulk environment, and a vacuum thickness of 1.0 nm is used to avoid interaction between repeated slabs. The bottom side of the slab is saturated with hydrogen atoms to prevent transfer of surface charges.

The calculation is taken with an energy cutoff of 400 eV. The convergence precision is set to energy change below 2×10^{-6} eV/atom, force less than 0.005 eV/nm, the convergence tolerance of a single atomic energy below 1×10^{-5} eV/atom, stress less than 0.05 GPa, and change in displacement less than 0.0002 nm in iterative process. All calculations are performed with a plane-wave pseudopotential^[11] method based on DFT combined with the generalized gradient approximation (GGA). The integral in the Brillouin^[12] zone is sampled with the Monkhorst-Pack^[13] scheme and special k points of high symmetry. The number of k points is $4\times 6\times 1$. All calculations are carried in reciprocal space with Ga:3d¹⁰4s²4p¹, and As:4s²4p³ as the valence electrons. The scissors operator correction was used for the optical properties calculation to ensure the calculation accuracy.

The As-rich $\beta_2(2\times 4)$ and Ga-rich (4×2) reconstruction models optimized by BFGS are shown in Fig. 1. Compare to the bulk, the thickness of the out-most bilayer of As-rich $\beta_2(2\times 4)$ surface increases by 29.9% and the thickness of the out-most bilayer of (4×2) surface decreases

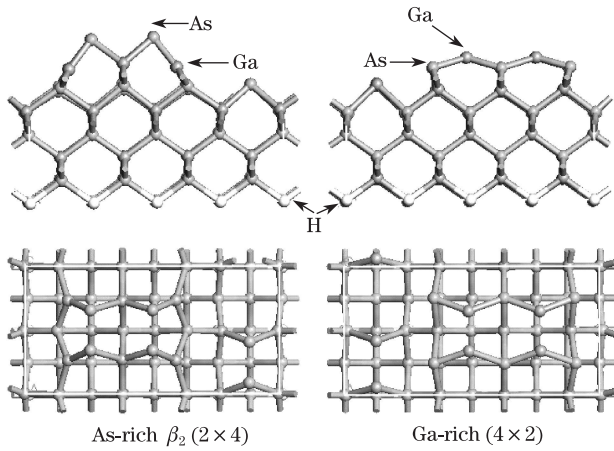


Fig. 1. (Color online) Side view and top view of As-rich $\beta_2(2 \times 4)$ and Ga-rich (4×2) reconstructions.

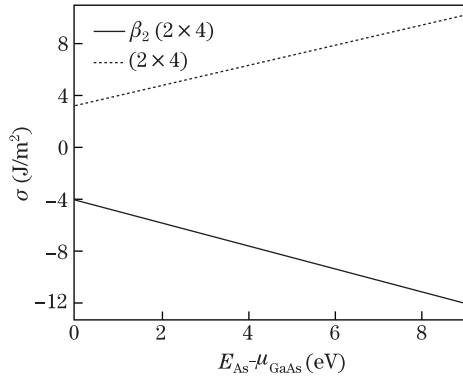


Fig. 2. Formation energy of As-rich $\beta_2(2 \times 4)$ and Ga-rich (4×2) reconstructions

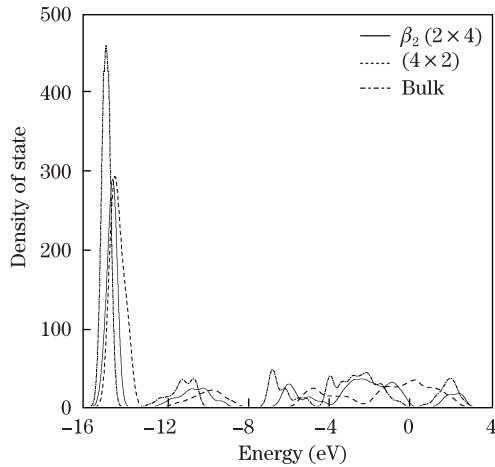


Fig. 3. Density of state of $\beta_2(2 \times 4)$ and Ga-rich (4×2) reconstructions

by 57.3%. The distance between Ga atoms of at the second layer of As-rich $\beta_2(2 \times 4)$ surface decreases by 15.0%, the distance between As atoms at the second layer of Ga-rich (4×2) surface increases by 10.9%. For the As-rich $\beta_2(2 \times 4)$ surface, the distance between the third layer of As and the fourth layer of Ga increases by 10.6%, and the relative distance for the Ga-rich (4×2) surface increases by 19.9%. The surface topography variation of Ga-rich (4×2) surface is more than the As-rich $\beta_2(2 \times 4)$ surface. The outmost atoms of As-rich $\beta_2(2 \times 4)$ surface

and Ga-rich (4×2) surface are As and Ga correspondingly, the valence bonds at the surface break up, and the dangling bonds is formed. The electrons without coordination are unstable. As atoms at the outmost of As-rich $\beta_2(2 \times 4)$ surface can form As-dimers to maintain the electric neutrality of the surface, while Ga-rich (4×2) surface can only maintain the electric neutrality by the variation of the surface. Thus the structure variation of Ga-rich (4×2) is more obvious.

Formation energy per unit area: σ is used to analysis the stability of the reconstruction surface. The σ is calculated by^[13,14]

$$\sigma A = E_{\text{slab}}^{\text{tot}} - N_{\text{Ga}}\mu_{\text{Ga}} - N_{\text{As}}\mu_{\text{As}}, \quad (1)$$

where $E_{\text{slab}}^{\text{tot}}$ is the total energy of the slab, N_{Ga} and N_{As} are relatively the number of Ga, As atoms, A is the area of surface, μ_{Ga} and μ_{As} are relatively the chemical potential of Ga, As atoms in the slab. μ_{Ga} and μ_{As} are constrained by $\mu_{\text{Ga}} + \mu_{\text{As}} = E_{\text{GaAs}}$, where E_{GaAs} is the GaAs chemical potential. The formula can be rewritten as

$$\begin{aligned} \sigma A &= E_{\text{slab}}^{\text{tot}} - N_{\text{Ga}}\mu_{\text{Ga}} - N_{\text{As}}\mu_{\text{As}} \\ &= E_{\text{slab}}^{\text{tot}} - N_{\text{Ga}}E_{\text{GaAs}} - (N_{\text{As}} - N_{\text{Ga}})\mu_{\text{As}}. \end{aligned} \quad (2)$$

μ_{As} satisfies

$$E_{\text{As}} - \mu_{\text{GaAs}} < \mu_{\text{As}} < E_{\text{As}}, \quad (3)$$

where E_{As} is the average energy of As atom in the As

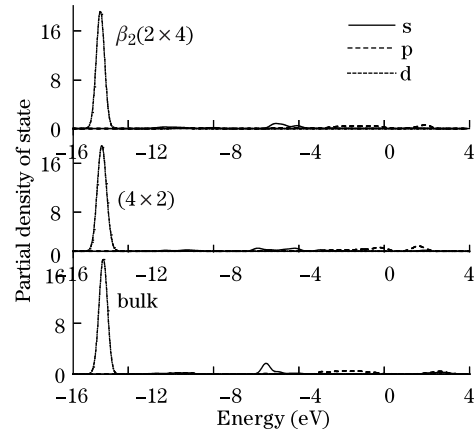


Fig. 4. Partial density of Ga atoms.

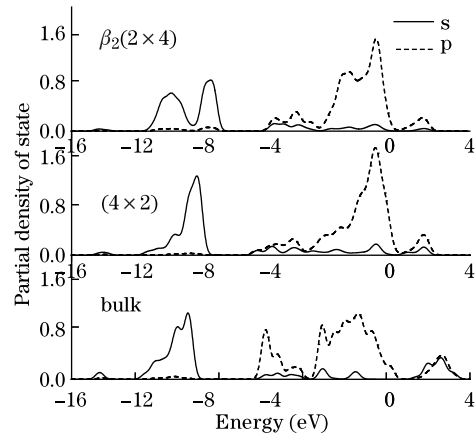


Fig. 5. Partial density of As atoms.

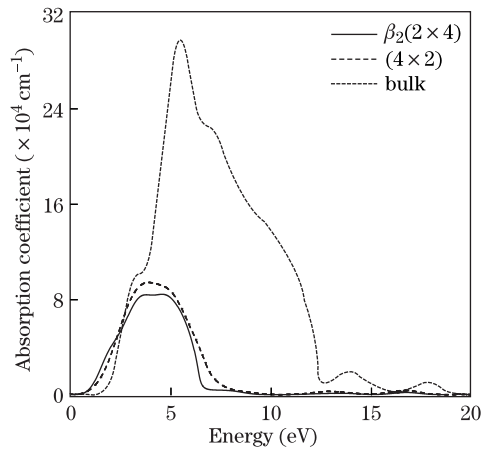


Fig. 6. Absorption spectra of reconstructions.

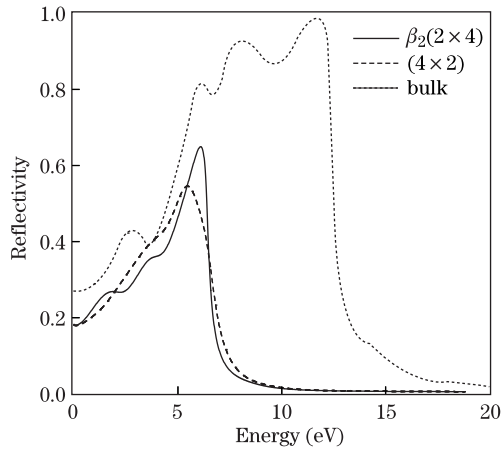


Fig. 7. Reflectivity spectra of reconstructions.

elementary substance, and μ_{GaAs} is the binding energy of the GaAs primitive cell. Figure 2 shows the formation energy of As-rich $\beta_2(2 \times 4)$ and Ga-rich (4×2) reconstructions. Result shows that the formation energy of As-rich $\beta_2(2 \times 4)$ reconstruction is minus and the formation energy of Ga-rich (4×2) reconstruction is positive, As-rich $\beta_2(2 \times 4)$ reconstruction is stable and Ga-rich (4×2) reconstruction is unstable.

For semiconductor, work function is defined as the minimum energy that electrons at the top of valence band escape to vacuum. Work function can be calculated by^[15]

$$\Phi = E_{\text{vac}} - E_f, \quad (4)$$

where E_{vac} is the vacuum energy, and E_f is fermi level. The calculated work function of As-rich $\beta_2(2 \times 4)$ and Ga-rich (4×2) reconstructions are 4.704 and 4.667 eV correspondingly. The band gap of GaAs is 1.42 eV, and Cs/O activation can reduce the electron affinity, thus leading to a NEA photocathode and improve the photoemission performance. The Ga-rich (4×2) reconstruction owns lower work function and is more easily to form NEA surface.

The density of state of As-rich $\beta_2(2 \times 4)$ and Ga-rich (4×2) reconstructions are shown in Fig. 3. Result shows that for reconstruction surfaces, the valence band consists of the lower valence band near -16.5 – -8.5 eV and upper valence band near -6.4 – 0 eV, and there are sharp

peaks near 14.25 eV, however for different reconstruction surfaces, the locations and the altitudes are different. Near the fermi energy level the integral density of state of the reconstruction surfaces are larger than that of the bulk. The conduction bands of reconstruction surfaces are closer to fermi energy level than the bulk. The fermi energy level of Ga-rich (4×2) reconstruction moves into the valence band and forms a strong localized state.

The integral density of state of As-rich $\beta_2(2 \times 4)$ and Ga-rich (4×2) reconstructions are calculated and compared to the integral density of state of GaAs bulk. Result shows that, the electrons of As-rich $\beta_2(2 \times 4)$ reconstruction decrease by 9.5% and the electrons of Ga-rich (4×2) reconstruction decrease by 22.9%. The electrons at the surface move into vacuum and form the “electron gas”. The potential caused by the “electron gas” blocks the escape of the photoelectrons. Electrons movement at Ga-rich (4×2) reconstruction is more than the As-rich $\beta_2(2 \times 4)$ reconstruction and the block effect of “electron gas” at Ga-rich (4×2) reconstruction is more obvious. This is because that As atoms at the outmost of As-rich $\beta_2(2 \times 4)$ surface can form As-dimers to maintain the electric neutrality of the surface, while Ga-rich (4×2) surface can only maintain the electric neutrality by the movement of electrons. As-rich $\beta_2(2 \times 4)$ is more benefit for photoelectron emission.

Figures 4 and 5 are the partial density of state of Ga atoms and As atoms respectively, The lower valence band is mainly formed by Ga 3d and As 4s state electrons, and there are sharp peaks of Ga 3d state electrons near -14.5 eV, which form strong localized states and are much larger than the strength of As 4s state electrons. The upper valence bands are mainly attributed to As 4p and Ga 4s state electrons; the top of the valence band is decided by As 4p state electrons. Conduction bands are mainly attributed to Ga 4s and Ga 4p state electrons and a small number of As 4p state electrons. The bottom of conduction bands are mainly decided by Ga 4s state electrons.

Compared to the bulk, the change of integral partial density of state of As-rich $\beta_2(2 \times 4)$ and Ga-rich (4×2) reconstructions are shown in Table 1, where the “-” means reducing and “+” means increasing. Result shows that, the Ga 3d state electrons are almost unchanged. For the As-rich $\beta_2(2 \times 4)$ reconstruction, the Ga 4s state and Ga 4p state decrease, and As 4s state, As 4p state, increase, while for the Ga-rich (4×2) reconstruction, Ga 4s state, Ga 4p state and As 4s state, As 4p state, all decrease. It is caused by that during the formation of the reconstruction surfaces, the isotropic sp^3 hybridized orbit would change to neutralize the dipoles moment and to maintain a steady surface. The change of Ga-rich (4×2) reconstruction is more obvious.

In the linear response range, the macro-optical response

Table 1. Variation of Electrons at Different Shells of Ga and As Atoms

	Ga		As		
	s	p	d	p	
As-rich $\beta_2(2 \times 4)$	-4.6%	-5.4%	+0.28%	+6.9%	+1.8%
Ga-rich (4×2)	-16.68%	-11.71%	+0.04%	-4.48%	-7.18%

functions of solids can be described by the complex dielectric function $\varepsilon(\omega) = \varepsilon_1(\omega) + i\varepsilon_2(\omega)$ or the complex refractive index $N(\omega) = n(\omega) + ik(\omega)$ ^[16], where

$$\varepsilon_1 = n^2 - k^2, \quad (5)$$

$$\varepsilon_2 = 2nk. \quad (6)$$

Absorption coefficient indicates the percentage of the light intensity decays during the spread through unit distance. Absorption spectra can be obtained by

$$\alpha \equiv 2\omega k/c = 4\pi k/\lambda_0. \quad (7)$$

The calculated absorption spectra of As-rich $\beta_2(2\times 4)$ reconstruction, Ga-rich (4×2) reconstruction and the bulk are shown in Fig. 6. After integral, we can get that the average absorption of As-rich $\beta_2(2\times 4)$ reconstruction is 19.5% of the bulk and the average absorption of Ga-rich (4×2) reconstruction is 23.2% of the bulk. The absorption band edges of these two surfaces both move to low-energy side. The absorption peaks of the bulk located at 3.1512, 5.1528 (maximum peak), 7.0900, 11.5613, 14.0632, and 17.7885 eV. The absorption peaks of As-rich $\beta_2(2\times 4)$ reconstruction located at 2.6152, 4.2856 (maximum peak), 6.7216, 10.5579, 11.9482, and 15.7191 eV. The absorption peaks of Ga-rich (4×2) reconstruction located at 2.2120, 3.1768 (maximum peak), 4.9322, 12.500, 13.3859, and 16.6944 eV. The absorption peaks of the reconstructions move to low-energy side and the peak values decrease. This is attributed to the variation of electrons distribution at shells of atoms near the surface.

The reflectivity spectra can be obtained by

$$R(\omega) = [(n-1)^2 + k^2]/[(n+1)^2 + k^2]. \quad (8)$$

The reflectivity spectra of As-rich $\beta_2(2\times 4)$ reconstruction, Ga-rich (4×2) reconstruction and the bulk are shown in Fig. 7. The static reflectivity of As-rich $\beta_2(2\times 4)$ and Ga-rich (4×2) reconstructions are smaller than the bulk. The falling edges of the reflectivity curves of the surfaces move to low-energy side. After integral, we can get that the average reflectivity of As-rich $\beta_2(2\times 4)$ reconstruction is 27.2% of the bulk and the average reflectivity of Ga-rich (4×2) reconstruction is 28.6% of the bulk.

The absorption and the reflectivity of the reconstructions are smaller than the bulk, thus the transmittance of the surface is larger than the bulk, which is helpful for the photons move through the surface to excite photoelectrons. Both the absorption and the reflectivity of As-rich $\beta_2(2\times 4)$ reconstruction are smaller than the Ga-rich (4×2) reconstruction. Thus the transmittance of As-rich $\beta_2(2\times 4)$ reconstruction is larger than that of Ga-rich (4×2) reconstruction. As-rich $\beta_2(2\times 4)$ reconstruction is more benefit for the movement of photos through the surface to emit photoelectrons.

In conclusion, using the first-principles plane-wave

pseudopotential method, based on the DFT, the formation energy, work function, density of state and optical properties of GaAs (100) $\beta_2(2\times 4)$ and GaAs (100) (4×2) reconstructions are calculated. The formation energy of As-rich $\beta_2(2\times 4)$ reconstruction is minus and the formation energy of Ga-rich (4×2) reconstruction is positive, As-rich $\beta_2(2\times 4)$ reconstruction is stable and Ga-rich (4×2) reconstruction is unstable. Ga-rich (4×2) reconstruction owns lower work function. The electrons at two reconstructions both move into the vacuum and form the “electron gas”. The “electron gas” of As-rich $\beta_2(2\times 4)$ reconstruction is less obvious and As-rich $\beta_2(2\times 4)$ is more benefited for photoelectric emission. Both the absorption and the reflectivity of As-rich $\beta_2(2\times 4)$ reconstruction are smaller than the Ga-rich (4×2) reconstruction. As-rich $\beta_2(2\times 4)$ reconstruction is more benefit for the movement of photos through the surface to emit photoelectrons.

This work was supported by the National Science Foundation of China under Grant No. 61171042.

References

1. L. I. Antonova and V. P. Denissov, *Appl. Surf. Sci.* **111**, 237 (1997).
2. D. A. Allwood, R. T. Carline, N. J. Mason, C. Pickering, B. K. Tanner, and P. J. Walker, *Thin Solid Films* **364**, 33 (2000).
3. Y. Z. Liu, J. L. Moll, and W. E. Spicer, *Appl. Phys. Lett.* **17**, 60 (1970).
4. D. Durek, F. Frommberger, T. Reichelt, and M. Westermann, *Appl. Surf. Sci.* **143**, 319 (1999).
5. L. Broekman, R. Leckey, J. Riley, B. Usher, and B. Sexton, *Surf. Sci.* **331-333**, 1115 (1995).
6. T. Hashizume, Q. K. Xue, J. Zhou, A. Ichimiya, and T. Sakurai, *Phys. Rev. Lett.* **73**, 2208 (1994).
7. Q. K. Xue, T. Hashizume, J. M. Zhou, T. Sakata, T. Ohno, and T. Sakurai, *Phys. Rev. Lett.* **74**, 3177 (1995).
8. H. P. Komsa, E. Arola, J. Pakarinen, C. S. Peng, and T. T. Rantala, *Phys. Rev. B* **79**, 115208 (2009).
9. L. H. Thomas, *Math. Proc. Camb. Phil. Soc.* **23**, 542 (1927).
10. Y. Du, B. Chang, X. Wang, J. Zhang, B. Li, and X. Fu, *Acta Phys. Sin.* (in Chinese) **61**, 057102 (2012).
11. J. P. Perdew, K. Burke, and M. Ernzerhof, *Phys. Rev. Lett.* **77**, 3865 (1996).
12. H. J. Monkhorst and J. D. Pack, *Phys. Rev. B* **13**, 5188 (1976).
13. J. E. Northrup and S. Froyen, *Phys. Rev. Lett.* **71**, 2276 (1993).
14. W. C. Wang, G. Lee, M. Huang, R. M. Wallace, and K. Cho, *J. Appl. Phys.* **107**, 103720 (2010).
15. A. L. Rosa and J. Neugebauer, *Phys. Rev. B* **73**, 205346 (2006).
16. Y. J. Du, B. K. Changa, H. G. Wang, J. J. Zhang, and M. S. Wang, *Chin. Opt. Lett.* **10**, 051601 (2012).